Original paper

Biomechan Model Mechanobiol 1 (2002) 151 – 164 © Springer-Verlag 2002
DOI 10.1007/s10237-002-0013-0

Brain mechanics For neurosurgery: modeling issues

Stelios K. Kyriacou, Ashraf Mohamed, Karol Miller, Samuel Neff

Abstract Brain biomechanics has been investigated for more than 30 years. In particular, finite element analyses and other powerful computational methods have long been used to provide quantitative results in the investigation of dynamic processes such as head trauma. Nevertheless, the potential of these methods to simulate and predict the outcome of quasi-static processes such as neurosurgical procedures and neuropathological processes has only recently been explored. Some inherent difficulties in modeling brain tissues, which have impeded progress, are discussed in this work. The behavior of viscoelastic and poroelastic constitutive models is compared in simple 1-D simulations using the ABAQUS finite element platform. In addition, the behaviors of quasi-static brain constitutive models that have recently been proposed are compared. We conclude that a compressible viscoelastic solid model may be the most appropriate for modeling neurosurgical procedures.

1
Introduction

The mechanical behavior of brain tissue is one of the most demanding and complicated to model. Depending on the application, viscoelastic (Miller 1999; Mendis et al. 1995; Wang and Wineman 1972), poroelastic (Paulsen et al. 1999; Miga et al. 1998a; Subramaniam et al. 1995; Kaczmarek et al. 1997; Pena et al. 1999; Nagashima et al. 1990; Tenti et al. 1999; Basser 1992) and even purely elastic (Kyriacou et al. 1999; Kyriacou and Davatzikos 1998; Takizawa et al. 1994; Ferrant et al. 2000) models have been used in different analyses. The characteristic time scale is very important for choosing the material model. Impact usually is modeled with viscoelasticity, while long term processes like hydrocephalus can be modeled using poroelasticity or mixture theory due to the need to account for interstitial fluid movement. In applications like brain image registration, even a purely elastic model may suffice.

Simulating the mechanical behavior of the human brain will be an important milestone in neurosurgery. One example is the following: neurosurgical retraction provides traction forces at the surface of the brain to provide a better field of view during microsurgical treatments such as clipping of skull base aneurysms. A complication of the retraction, however, may be neurological impairment due to a retractor-induced injury to the tissue (Yundt et al. 1997). Thus, a reasonably accurate simulation tool to predict the level of stress within the tissue would be of high value. More specifically, a biomechanical model of brain anatomy could be used to optimize retractor-applied pressure and

Received: 19 March 2002 / Accepted: 6 June 2002

S. K. Kyriacou (✉), A. Mohamed
Department of Radiology and Radiological Science
The Johns Hopkins University, Baltimore, Maryland
e-mail: kyriacou@cbmv.jhu.edu

K. Miller
Department of Mechanical and Materials Engineering
The University of Western Australia, Perth

S. Neff
Neurosurgery, St. Christopher's Hospital for Children,
Philadelphia, Pennsylvania

Work is supported by a generous grant from the Whitaker Foundation. We would like to also thank Dr. Christos Davatzikos (Johns Hopkins School of Medicine, Baltimore, Maryland) for his help.

retractor-position to achieve an adequate field of view while avoiding injury to tissue from retraction strains.

In this paper, we discuss and propose solutions to important questions concerning the quasi-static biomechanical behavior of brain tissues. Some of the issues considered are: poroelastic vs. viscoelastic and compressible vs. incompressible material behavior, a fluid vs. solid approach, differentiating between gray and white matter properties, the effect of tissue weight, fluid filled cavities (ventricles, subarachnoid space) and falx/tentorium, and the issue of mesh generation. Also, different constitutive models are compared under various simple 1D simulations.

2 Modeling Issues

Brain anatomy and physiology

The human brain is a soft yielding structure that is not as stiff as a gel or as plastic as a paste (Ommaya 1968; Goldsmith 1972; Akkas 1979). The soft tissue consists of gray matter, containing neuronal cell bodies, and white matter, containing interconnecting fibers between areas of gray matter (Fig. 1). The soft tissue is covered by the dura, arachnoid, and pia membranes, with the space between the arachnoid and pia (subarachnoid space) filled with the cerebrospinal fluid (CSF), a clear, colorless fluid. The subarachnoid space communicates with the four ventricles which are cavities filled with CSF.

Constitutive models for brain tissue

Constitutive models are attempts to quantify the behavior of materials under different loading conditions. Decisions on which specific model to use must be based on observed responses to these loading conditions as well as on our knowledge of structure and histology. As we already mentioned, the mechanical behavior of brain tissue may be modeled in different ways based on the specific conditions of interest and in particular on the magnitude of the strain rate. Hence, different constitutive relations may be needed for the same material depending on the particular condition.

We will restrict our discussion to elastic, viscoelastic, and poroelastic (or mixture theory) constitutive relations. An elastic behavior may be defined as one in which the stress state depends only on strain; a viscoelastic behavior may be defined as one that the stress state depends both on strain and strain history; a poroelastic behavior may be defined as one that results from two or more phases, with one phase being an elastic solid and the other being a fluid.

Currently, investigators are using different models and material parameters to study the following processes: 1. Quasi-static[1] processes (e.g. neurosurgical retraction, brain shift during surgery, hematomas, hydrocephalus etc.) are simulated by mostly poroelastic (Paulsen et al. 1999; Miga et al. 1998a; Miga et al. 2000; Subramaniam et al. 1995; Kaczmarek et al. 1997; Pena et al. 1999; Nagashima et al. 1990; Tenti et al. 1999; Basser 1992), viscoelastic (Miller 1999), or nonlinear elastic (Sahay et al. 1992) and even linearly elastic models (Ferrant et al. 2000; Skrinjar et al. 2001; Skrinjar and Duncan 1999). Paulsen's group (Paulsen et al. 1999; Miga et al. 1998a; Miga et al. 2000) used a poroelastic model (linear material and strain) to evaluate intraoperative brain shift for image corrections during image guided surgery, and recover 80% of deformation under loads compared to clinical conditions. Ferrant et al. 2000 used a linear elastic material and linear strain for similar purposes of evaluating brain shift. Skrinjar and colleagues (Skrinjar et al. 2001; Skrinjar and Duncan 1999) used both a linear mass spring (discrete) model and a linear (both material and strain linearity) elastic continuum model for evaluating brain shift. Nagashima and colleagues (Nagashima et al. 1994; Nagashima et al. 1990; Nagashima et al. 1990; Nagashima et al. 1987) used a linear material and linear strain with a 2D FEM-based poroelastic theory. This allowed them to model edema as well as to investigate issues like hydrocephalus. Neff and collaborators (Subramaniam et al. 1995; Kaczmarek et al. 1997) used a similar 2D poroelastic model with a nonlinear strain definition and a linear material to numerically study the biomechanics of hydrocephalus and other structural neurologic diseases. 2. Impact (e.g. during falls or car accidents) has been studied mostly via linear viscoelastic (Bandak et al. 1995; Wang and Wineman 1972), or nonlinear viscoelastic (Donnelly and Medige 1997; Mendis et al. 1995; Bilston et al. 1997) models. Miller's group (Miller 1999; Miller and Chinzei 1997; Chinzei and Miller 1996; Miller et al. 2000) developed a viscoelastic model to simulate both quasi-static and fast (up to a strain rate of

[1] By quasi-static processes, we refer to slow enough processes for the mass-acceleration term to be negligible, for example when strain rates are slower than 0.1 s^{-1}. On the other hand, strain rate will still be included for calculating stresses in the viscoelastic constitutive relation.

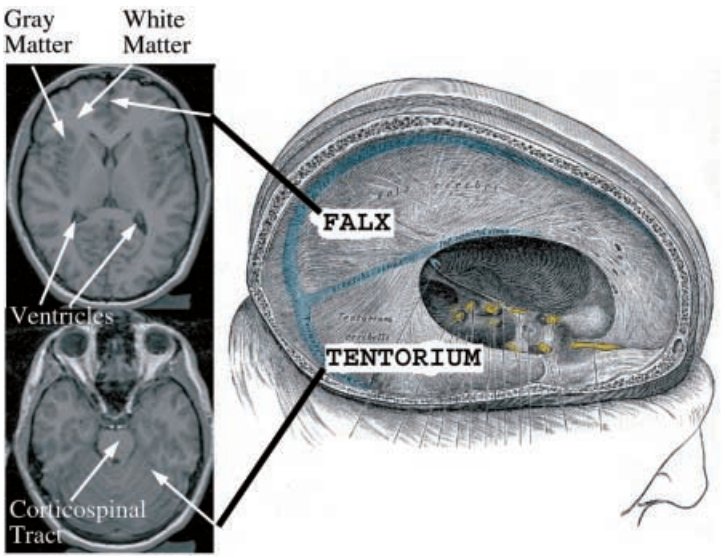

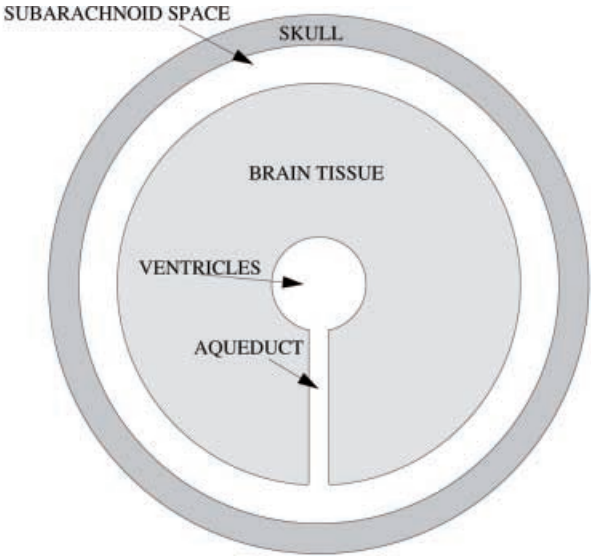

Fig. 1. An illustration of some major features of the anatomy of the human brain. Left and middle panels: The falx and tentorium membranes divide the brain into the two cerebral hemispheres and the cerebellum; they are relatively stiff membranes, and they constrain the potential deformations of the soft tissue. The parenchyma is composed of white and gray matter; ventricles are cavities that are filled with cerebrospinal fluid. Right panel: a simplified schema of the connection between the subarachnoid space and ventricles; features have been exaggerated for illustrative purposes. (middle panel from Bartleby.com by permission.)

0.64 s^{-1}) processes. In addition to material experimentation and model development, they simulated an experiment on live swine brain using ABAQUS, but forces were found to be 31% lower than reality. This discrepancy may be due to the use of generic swine material properties rather than specific to the individual experimental animal.

In addition to the use of biomechanical brain models for simulating neurosurgical procedures and neurological processes, brain biomechanics has been used to match/register two brain volumes from two different individuals based on material properties and boundary conditions as well as image intensities. For example, we and others (Kyriacou et al. 1999; Wasserman and Acharya 1996) used nonlinear hyperelastic or linear models respectively to register an anatomical atlas to a tumor-bearing brain image volume.

Compressible vs incompressible model

The issue of compressibility of brain tissue warrants careful investigation because the tissue may behave incompressibly in impact situations while it may be effectively compressible in long duration processes (Kaczmarek et al. 1997). Furthermore, fluid cavities like the ventricles and subarachnoid space, and their interconnections, allow movement of fluid and thus apparent changes of local volume (Sarron et al. 2000). Also, many brain models do not include the ventricular and subarachnoid cavities. Thus, it may be prudent to use a compressible material. On the other hand, Miller and Chinzei (1997) have not observed volume changes in their 1-D compression experiments although a rigorous measurement of the volume change was unsuccessful due to technical reasons. Thus, the model by Miller et al. (2000) invokes incompressibility to simulate the deformation in swine brain even for quasi-static processes such as surgical manipulations. On the other hand, the poroelastic model is by definition compressible in an aggregate sense (even though the constituents are both incompressible) so that it will allow fluid movements. In the case that the fluid movement is not of importance, it may be prudent to use a relatively simpler viscoelastic model (compared to a poroelastic model) and to calculate an appropriate viscoelastic compressibility term from the poroelastic model through use of simple simulations (an example is described in the Results section). Compressibility constants have been calculated by various groups. Some groups used a linear poroelastic material: Tenti et al. (1999) calculated a dry Poisson's ratio $\nu = 0.4$ based in part by reevaluating the data by Metz et al. (1970). Miga et al. (1998b) used an approximate value of $\nu = 0.45$ chosen from a range that minimized errors in their experiments. These experiments consisted of inflating a balloon inside a porcine brain and measuring the displacement of inserted beads. Other groups used a linear elastic material (with possibly a viscous component): Guillaume et al. (1997) found that a $\nu = 0.35$ gives best agreement with hypergravity experiments on excised bovine brains. Skrinjar et al. (2001) tried different values for ν so as to minimize errors between intraoperatively acquired data and calculated results; they found that $\nu = 0.4$ gives optimal results. Nevertheless, there seems to be an absence of rigorous experimental work for finding brain tissue compressibility, either in vitro or even more importantly in vivo.

Another variable of interest in modeling neurosurgical procedures is the use of mannitol and other diuretics which have the effect of reducing the brain volume. Thus, the use of such drugs should also be modeled by applying a corresponding brain tissue volume reduction.

Fluid vs solid model

Bilston et al. (1997) suggested that brain tissue lacks a long term elastic modulus and thus it is a fluid. Shuck and Advani (1972) seem to agree since they found that a viscoelastic fluid represents the material behavior of brain better than a viscoelastic solid. But Donnelly and Medige (1997) reported that brain tissue samples, immersed in saline, return to a clearly defined shape after being deformed, which indicates a need for a solid model. Nevertheless, this characteristic was not so evident when the tissue was removed from saline. In addition, Shuck and Advani (1972) discuss yield properties of brain tissue; this would strengthen the solid model theory since fluid models are not usually associated with yield. One possible explanation for these apparent disagreements may be that experimental data in Bilston's work went down to a modulus of approximately 800 Pa while Miller's data show a long term modulus of approximately 500 Pa for small strains. Another useful constitutive model for brain tissue may be the elastoplastic material. This would justify the contradiction that brain tissue behaves as an elastic solid when immersed in saline and as a fluid when not immersed in saline. The gravity forces on the tissue when not immersed may be larger than the yield point of the elastoplastic behavior so that the tissue seems to be a fluid under those conditions.

Gray vs white matter elastic properties

According to Bilston et al. (1997), some researchers found no difference between the elastic properties of the white and gray matter while others did find differences. Nagashima et al. (1990)

assumed a much stiffer (10-fold) gray matter without fully justifying their choice. Kaczmarek et al. (1997) used the same elastic properties for both white and gray matter, taken from the lowest strain tests performed by Metz et al. (1970). Nevertheless, they also tried sensitivity analysis simulations with the gray matter taking values of increasing stiffness, starting from a stiffness the same as that of the white matter and ending at a stiffness four times larger, based on their expectation that gray matter is stiffer than white matter. Ozawa et al. (2001) performed experiments on rabbit spinal cord (whose material properties may differ from brain's) and showed no significant difference in stiffness between gray and white matter. Prange et al. (2000) investigated the effect of regional, directional, and species effects on brain mechanical properties. They found that gray matter (thalamus) was in an average sense stiffer than white matter (corona radiata and corpus callosum) by about 30% in fresh swine brain tissue. In addition they found directional dependence of stiffness in the white matter (about 70% stiffer in the second direction) and to a much lesser extent in gray matter (about 10% stiffer in second direction). Due to this anisotropy, the white matter stiffest direction may be stiffer than the gray matter stiffest direction. Zhou and collaborators (Zhou et al. 1994; King et al. 1995) used a 60% stiffer white matter due to its fibrous nature. Manduca et al. (2001) reported that Magnetic Resonance Elastography (which is a very promising though not fully mature technique for measuring shear moduli) showed a stiffer white matter with an average shear stiffness of 14.2 kPa while gray matter average shear stiffness was 5.3 kPa. There seems to be a need for further experimentation even though the work by Prange et al. (2000) seems most convincing.

Effect of gravity and CSF submersion

Gravity may be an important modeling force due to the very low stiffness of brain tissue. Since the brain is submerged in CSF in physiological conditions, its weight is neutralized by the fluid pressures (buoyant force). This is important in neurosurgical navigation during open skull surgery where loss of CSF seems to be the dominant factor in inducing an average of 10 mm of deformation mostly along the direction of gravity (Roberts et al. 1998). Thus, it is clear that modeling the weight of brain tissue and taking the weight into account when doing compression experiments for finding the material properties is important, especially when the height of the specimen is relatively large.

Importance of subarachnoid gap and falx/tentorium

The size of the subarachnoid gap has been modeled as having zero thickness for the lower half of the skull (due to settling) and having a linearly increasing gap for the upper half of the skull with maximum gap being 0.75 mm (Miller et al. 2000). Two extensions of the tough dura membrane, the falx and tentorium, are important since they provide a boundary for the various compartments of the brain such as the two hemispheres and the cerebellum. Nevertheless, these membranes are not always taut, and can even be calcified, so modeling them may be especially difficult.

Mesh generation for medical images

Mesh generation (and application of boundary conditions) is a challenging issue in biomechanical models since there is high variability in human anatomies; thus, mesh generation has to be tailored to each individual brain. In addition, the human brain has many intricate morphological details (e.g. the ventricular shape) that add further complications in model creation. An additional difficulty is that the anatomy is often revealed via an MRI or CT volume image that needs to be translated into a geometrical model for meshing. Widely used image processing, solid modeling, and FEM commercial software have not made the modeling process any easier. Only MIMICS (Materialise, Ann Arbor, MI) seems to have a mostly automated method to go from the image volume to a CAD model (IGES NURBS surfaces) for creating the FE model. Nevertheless its cost makes it rather expensive for academic research. In addition, it is only available for the windows platform. Analyze (Mayo Foundation, Rochester, MN), a commercial software that is widely used in academic environments and is compatible with Unix workstations, has an IGES output for points but not surfaces, thus further processing is required to created CAD models. Thus, in-house semi-automated and fully-automated methods for model generation have been investigated by many brain modeling researchers: Miller et al. (2000) used a semi-automatic mesh generation by first defining section contours on each volumetric section and then created the 3D geometry and FE model within MSC-PATRAN (MSC.Software Corporation). Ferrant et al. (2000), Miga et al. (1998b), and Hartmann and Kruggel (1999) have written automatic mesh generation software and used it to create anatomically correct brain models. Our group has also developed an automated mesh generator, which will be described in a separate publication.

3
Methods

Due to the complexities of the material behavior and contact constraints that will be needed for a full 3D brain biomechanical model, we used ABAQUS, which has a rich library of constitutive models and efficient contact interfaces. We tested the various brain material models by computing the solution of a simple boundary value problem, motivated by the standard uniaxial compression experiments described in Miller and Chinzei (1997), which may be the only quasi-static data we have on brain tissue to date. The geometry for this boundary value problem is a cylindrical specimen loaded along its axis of symmetry by a uniform pressure, with zero friction at the top and bottom surfaces (see figure 2). Its unloaded dimensions are a diameter of 30 mm and a height of 13 mm. The experiment was modeled in an axisymmetric fashion with the bottom having no displacement in the z direction and no displacement in the x direction at the symmetry axis. The element used was the ABAQUS axisymmetric 8-node biquadratic displacement, bilinear pore pressure (for poroelastic models), hybrid (for incompressible models), reduced integration element (CAX8RP for poroelastic, CAX8RH for incompressible and CAX8R for compressible viscoelastic). The number of elements was just 1 for homogeneous solutions and approximately 200 for inhomogeneous solutions (i.e., the poroelastic solutions with side flow). In the second case of inhomogeneity, stresses reported here were average quantities over the circular cross-section of the simulated cylindrical shape.

We performed the following simulations.

- Constant speed simulations: the top surface was compressed at two constant speeds: 8.3333E-8 m/s (strain rate of 6.41E-6 s^{-1}) for 50,000 s, which corresponds to the slowest speed experiment in (Miller, Chinzei 1997) and 8.3333E-3 (strain rate of 6.41E-1 s^{-1}) for 0.5 s, which corresponds to the fastest speed experiment in Miller. In both cases, the final stretch ratio was 0.68.
- Stress relaxation (constant displacement) simulations: the top surface was compressed (in a "ramp" fashion) by a constant strain in 0.02 s and then kept there for 1000 s (unless mentioned otherwise). This compressive strain was approximately –0.2307 (3 mm displacement).

The following constitutive models were compared under the above simulated experiments.

- Viscoelastic constitutive model: this is a single integral, finite strain, viscoelastic, isotropic model, based on a generalized Mooney-Rivlin elastic response and a relaxation response based on a Prony series expansion. The potential function W is in the form of the following convolution integral (Miller 1999; ABAQUS 2001):

$$W = \int_0^t \left\{ \sum_{i+j=1}^{N} C_{ij}(t-\tau) \frac{\mathrm{d}}{\mathrm{d}\tau} \left[(\bar{I}_1 - 3)^i (\bar{I}_2 - 3)^j \right] + \sum_{i=1}^{N} (1/D_i(t-\tau)) \frac{\mathrm{d}}{\mathrm{d}\tau} \left[(J-1)^{2i} \right] \right\} \mathrm{d}\tau \qquad (1)$$

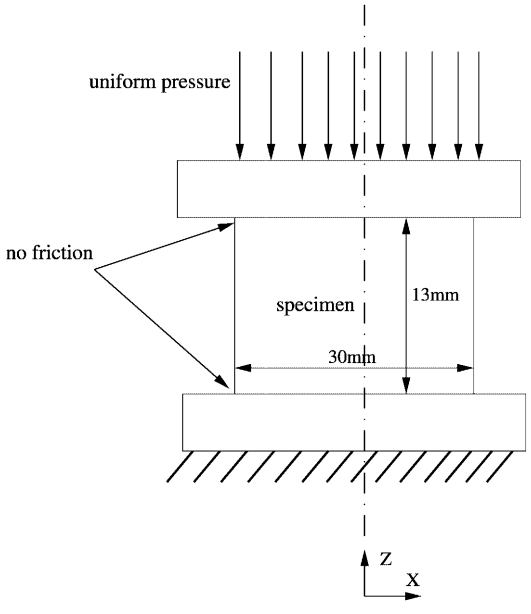

Fig. 2. Simulated experiment setup

where

$$\bar{I}_1 = J - (2/3)I_1, \quad \bar{I}_2 = J - (4/3)I_2, \quad I_1 = \lambda_1^2 + \lambda_2^2 + \lambda_3^2, \quad I_2 = \lambda_1^{-2} + \lambda_2^{-2} + \lambda_3^{-2}$$

and J is the volume ratio (i.e. $det(\mathbf{F})$, the determinant of the deformation gradient). The shear and compliance relaxation moduli functions C_{ij} and D_i are in the form:

$$C_{ij} = C_{ij0}\left(1 - \sum_{k=1}^{n} g_k\left(1 - e^{-t/\tau_k}\right)\right)$$

$$D_i = D_{i0}\left(1 - \sum_{k=1}^{n} k_k\left(1 - e^{-t/\tau_k}\right)\right)$$

where C_{ij0},D_{i0} are the instantaneous shear and compliance moduli, τ_k,g_k,k_k are the characteristic times, shear, and compliance relaxation coefficients, respectively, and t is the time. We used the following material parameters for fresh swine brain tissue behavior that were shown to model quasi-static conditions with good accuracy (Miller 1999): The non-zero stiffness coefficients were $C_{100} = C_{010} = 263$ *Pa*, $C_{200} = 491$ *Pa*, $C_{020} = 491$ *Pa*, *and* $C_{110} = 0$ *Pa*. The two characteristic times τ_k (for k = 1, 2) and related shear relaxation coefficients g_k were $\tau_1 = 0.50$ *s*, $g_1 = 0.450$, $\tau_2 = 50.0$ *s*, *and* $g_2 = 0.365$ (note that a zero value for the shear or compliance relaxation coefficients indicates zero viscous effects in the shear or compliance moduli respectively, while a unity value would indicate moduli that diminish to zero at infinite time). Values for D_{i0} were assumed to be zero (signifying incompressibility) unless otherwise noted (and thus k_k were not required). In the simplest case of non-zero D_{10} with $k_1 = 0$, the correspondence of the initial bulk modulus K_0 to D_{10} is well known (ABAQUS 2001): $K_0 = 2/D_{10}$

- Poroelastic constitutive model. This is a finite strain, poroelastic, isotropic model based on linear (material-wise) elastic response (ABAQUS 2001; Kaczmarek et al. 1997)[2] : The total stress tensor is given by the effective stress σ^e minus the hydrostatic pressure $P_i\boldsymbol{I}$ (by definition a positive quantity): $\sigma=\sigma^e-P_i\boldsymbol{I}$. Also needed is Darcy's Law: $\mathbf{U} = -K\nabla P_i$, where $\mathbf{U}$ is the velocity of the fluid and K is the hydraulic conductivity. Finally, mass conservation requires $\nabla(\phi\mathbf{U}) = 0$, where ϕ = the interstitial fluid fraction (Kaczmarek et al. 1997, which is assumed to be a constant.
  Assuming the elastic skeleton is isotropic and linearly elastic, the effective stress will be:

  $$\sigma^e = 2G\varepsilon + \lambda tr(\varepsilon)\mathbf{I} \ .$$

  The shear modulus G and λ are the Lamé constants with the standard relations to the Young's modulus E and Poisson's ratio v. E = 3156 Pa, based on the instantaneous modulus in Miller's viscoelastic model, calculated as follows: Shear modulus $G = 2 \cdot (C_{100} + C_{010}) = 2 \cdot (263 + 263)$ *Pa*; based on Miller's assumption of incompressibility and thus assuming a nominal $v = 0.5$, Young's modulus $E = G \cdot (2(1 + v)) = 3156$ *Pa*. The rest of the parameters are based on Kaczmarek et al. (1997): dry solid $v = 0.35$, K = 1.6E−11 m^4/(Ns). Note that, for ABAQUS compatibility, we assumed an initial $\phi = 0.22$; this value should not affect the stress and strain results since we have not allowed change of permeability with ϕ in the "permeability" section of the ABAQUS input file.
- Generalized Mooney-Rivlin constitutive model: This model and the material parameters are exactly the same as the hyperelastic part of the viscoelastic model above:

  $$W = \sum_{i+j=1}^{N} C_{ij}(\bar{I}_1 - 3)^i(\bar{I}_2 - 3)^j + \sum_{i=1}^{N}(1/D_i)(J-1)^{2i}$$

- Neo-Hookean constitutive model: $W = \mu(I_1-3)$, with μ based on the instantaneous modulus in Miller's viscoelastic model ($\mu = C_{10} + C_{01}$). Thus, $\mu = 526$ *Pa*. Incompressibility was assumed.
- Linear constitutive model:

  $$\sigma = 2G\varepsilon + \lambda tr(\varepsilon)\mathbf{I} \ ,$$

[2] This formulation allows finite strain in contrast to work by Paulsen's group (Paulsen et al. 1999, Miga et al. 1998a) which does not.

which is also based on the instantaneous modulus in Miller's viscoelastic model. Thus, E = 3156 Pa. A nearly incompressible behavior was assumed with $\nu = 0.4999$.

The resulting boundary value problems were solved by imposing force equilibrium with $\nabla \cdot \sigma + \mathbf{F} = \mathbf{0}$. Finite strain (NLGEOM keyword in ABAQUS) was used throughout.

We would like to clarify that while the viscoelastic model is fully nonlinear, the poroelastic one is only strain-wise nonlinear. This was partly dictated by our decision to use the ABAQUS platform for our simulations which does not readily allow a nonlinear poroelastic model. A justification for comparing these two not so similar models is that both formulations have already been used to model neurosurgical procedures (Miller et al. 2000; Paulsen et al. 1999).

4 Results

Validation

Validation in computational mechanics is key to successful modeling; numerical convergence alone is not sufficient. One such validation was to compare the results of 1D constant speed compression for our neo-Hookean ABAQUS-based model against analytical results (patch tests). In particular for $\mu = 15000$ Pa and an axial stretch ratio $\lambda = 0.67949$, the stress along the compression axis was analytically calculated to be: $\sigma = -30300$ Pa, which matched perfectly the ABAQUS solution. In addition, the results from the viscoelastic model were tested against analytical results from (figs. 3b and 3c) Miller (1999) and found to be in excellent agreement.

Nomenclature used in the various plots:

- **viscoel**: The viscoelastic model as explained in Methods.
- **poroel_NF**: The poroelastic model as explained in Methods with zero boundary flow conditions (NF stands for No Flow).
- **poroel_NF_P0**: The poroelastic model as explained in Methods with zero boundary flow conditions and a zero bulk pressure condition so as to imitate the behavior of the drained solid (P0 stands for zero Pressure).
- **poroel_SF**: The poroelastic model as explained in Methods with free flow (zero pressure) boundary conditions on the sides of the cylinder (SF stands for Side Flow).
- **poroel_SF_kaczmarek**: A similar poroelastic model, but with a value for E taken from Kaczmarek et al. (1997) rather than based on the instantaneous E from Miller's model: E = 10000 Pa.
- **poroel_SF_miga2000a**: A similar poroelastic model, but with parameters based on Miga et al. (2000): E = 2100 Pa, $\nu = 0.45$, and K = 1.0E−7 $m^4/(Ns)$.
- **mooney_N2**: The generalized Mooney-Rivlin model as explained in Methods (N2 stands for N = 2).
- **neohook**: The neo-Hookean model as explained in Methods.
- **miller_1997_low**: Digitized experimental data for low speed compression of swine brain tissue from Miller and Chinzei (1997) (included for comparison purposes).
- **miller_1997_high**: Digitized experimental data for high speed compression of swine brain tissue from Miller and Chinzei (1997) (included for comparison purposes).

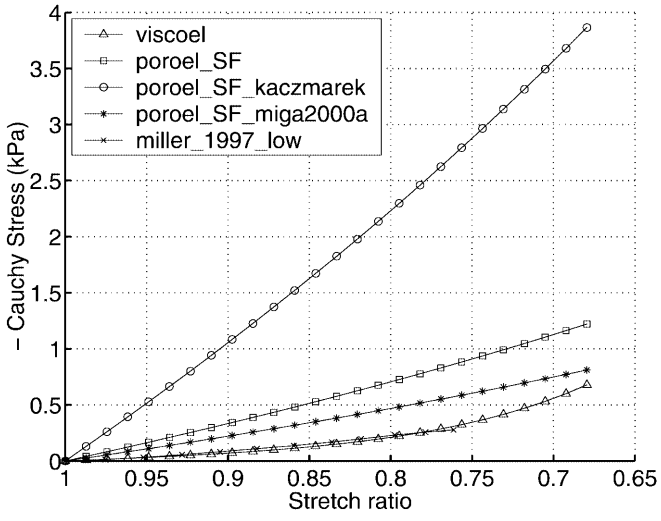

Fig. 3. Cauchy stress vs stretch ratio for four constitutive models that have been proposed recently for quasi-static modeling of brain tissue. The results are for the slow constant speed compression of a cylindrical shape. The "poroel_SF_kaczmarek" is based on a poroelastic model with side flow and material properties based on Kaczmarek et al. (1997). The "poroel_SF_miga2000a" is based on Miga et al. (2000). The "poroel_SF" and the "viscoel" are poroelastic and viscoelastic models respectively based on Miller (1999)

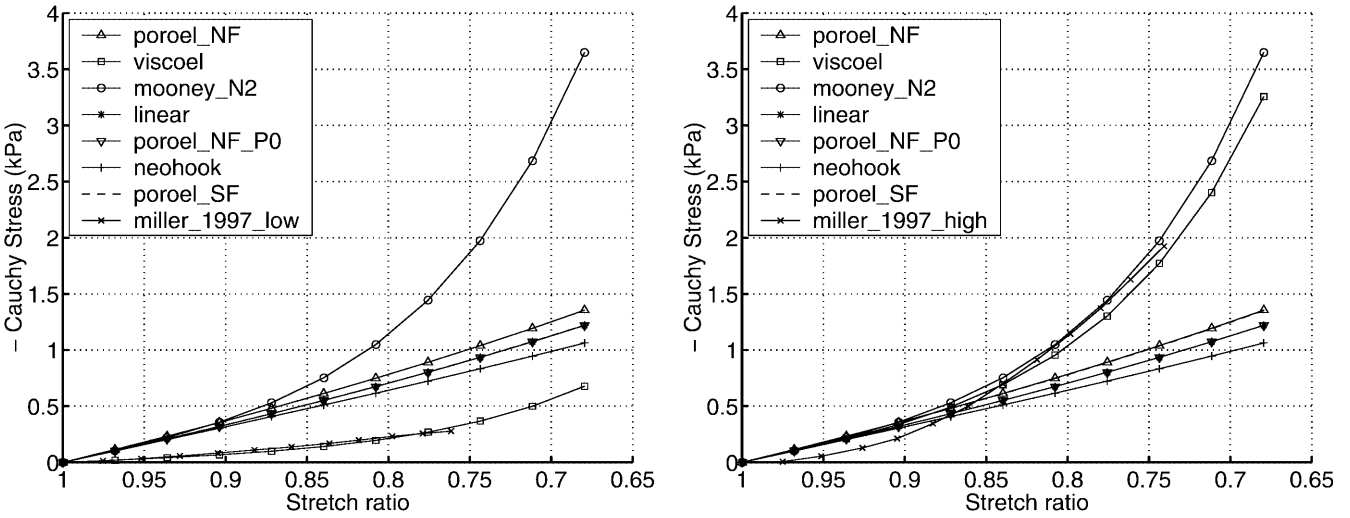

Fig. 4. Cauchy stress vs stretch ratio for various models based on the same instantaneous elastic modulus. Left: low speed of –8.3333E-08 m/s; the viscoelastic model has the softest response due to relaxation. The mooney_N2 shows a strong stiffening effect at approximately 0.85 stretch ratio. The poroel_SF, the poroel_NF_P0 and the linear model behavior coincide partly due to the fact that the fluid does not affect the stress due to the slow speed. Right: high speed of –8.3333E-03 m/s. As expected, most models have the same instantaneous stiffness at small strains. The only exceptions are the poroel_NF and poroel_SF which have an approximately 11% higher stiffness (although not clearly visible in this plot) since the Young's modulus and Poisson's ratio are for the drained solid matrix, and the fluid presence adds some extra stiffness. Both poroel_SF and poroel_NF behaviors coincides since fluid does not have time to move due to the high speed. The drained matrix behavior was given by the poroel_NF_P0 whose behavior coincides with the linear behavior

Low speed compression: Behavior of various proposed models
Figure 3 shows the behavior of the simulated cylindrical specimen under various constitutive behaviors proposed by different groups in the last few years. Three different poroelastic materials (with free side flow) and a viscoelastic one were tested in low speed compression. The results show that for the poroelastic materials the Young's modulus seems to be the dominant player that decides their behavior in 1D compression.

Constant speed compression: Behavior of models based on Miller's instantaneous elastic modulus
We compared the behaviors of various models that had their initial instantaneous elastic modulus based on Miller's model. Results are presented in figure 4 for constant speed compression. The absolute Cauchy stress is plotted against the stretch ratio. The solution is homogeneous except for the case of the side flow poroelastic model. In that case, as we mentioned earlier, the stress is an average, calculated on the top of the specimens by summing all the reaction forces on the top nodes of the specimen and dividing by the total deformed top surface area.

A Compressible viscoelastic model
We tested the poroelastic model poroel_SF for compressibility under stress relaxation, with results shown in figure 5, right panel. Volume reduction seemed to converge to about 7.5%. There was no effect when the void ratio was changed from 0.22 to 0.05. We also tested the viscoelastic model with different degrees of compressibility D_{10} (for simplicity, keeping $k_1 = 0$) and compared the percent volume compression at the end of the slow constant speed simulation to that of the poroelastic model. We found that a $D_{10} = 0.00110\ \text{Pa}^{-1}$ seems to give the same percent volume compression (ratio of final to initial volume) equal to 10.8%. Figure 5, left panel, shows the compressibility for the whole time period. The right panel shows the behavior of the two models under stress relaxation. Obviously, this is a rather simplistic approach for finding an equivalent viscoelastic compressibility, so further investigation is required.

Relaxation simulation
We tested the side flow poroelastic and the viscoelastic models under stress relaxation (figure 6). The results show a much less pronounced relaxation behavior for the side flow poroelastic model compared to the viscoelastic model. For comparison purposes, we also plotted the Mooney-Rivlin and the no-flow poroelastic models even though they do not change with time (the first because it is hyperelastic and the second because fluid is not allowed to leave).

5
Discussion
We have discussed important issues in brain biomechanical modeling such as the appropriateness of using poroelastic vs. viscoelastic constitutive models, the compressibility of the tissue, the use of fluid vs. solid models, etc. In addition, we have compared the behavior of various constitutive models that have been proposed in the literature.

We conclude that a good way to model neurosurgical retraction (while other conditions may require a different type of modeling) may be the following: if there is no specific requirement for knowing the interstitial fluid movement, use the viscoelastic model developed by Miller's group for the whole brain; in addition allow for a compliance modulus (compressibility response) that initially may be based on the compliance modulus of previously proposed poroelastic models, until more complete data on the compressibility of brain tissue in-vivo become available. A solid model may be more appropriate than a fluid model even though a very low equilibrium modulus may be necessary. Another possibly useful model may be the elastoplastic model which would handle the possibility of material yielding by the applied stress. We propose the use of same stiffness for both the white and gray matter as a first approximation, since experimental work has been inconclusive. A subarachnoid gap based on Miller's work that increases linearly from zero width to a maximum width of 0.75 mm at the highest brain position may be used as a first approximation.

We have shown how the behavior of the poroelastic model compares to the viscoelastic one proposed by Miller in simple 1-D simulations of experimental procedures used to evaluate brain tissue properties. The poroelastic model has a Young's modulus derived from the instantaneous elastic response of the viscoelastic model. The viscoelastic model showed a much stronger dependence on strain rate than did the poroelastic model (figure 4). Similarly, stress relaxation was much more pronounced in the viscoelastic model compared to the poroelastic model (figure 6). This agrees with observations by Miller (1998). On a similar note, it has been postulated that many viscoelastic phenomena like creep and stress

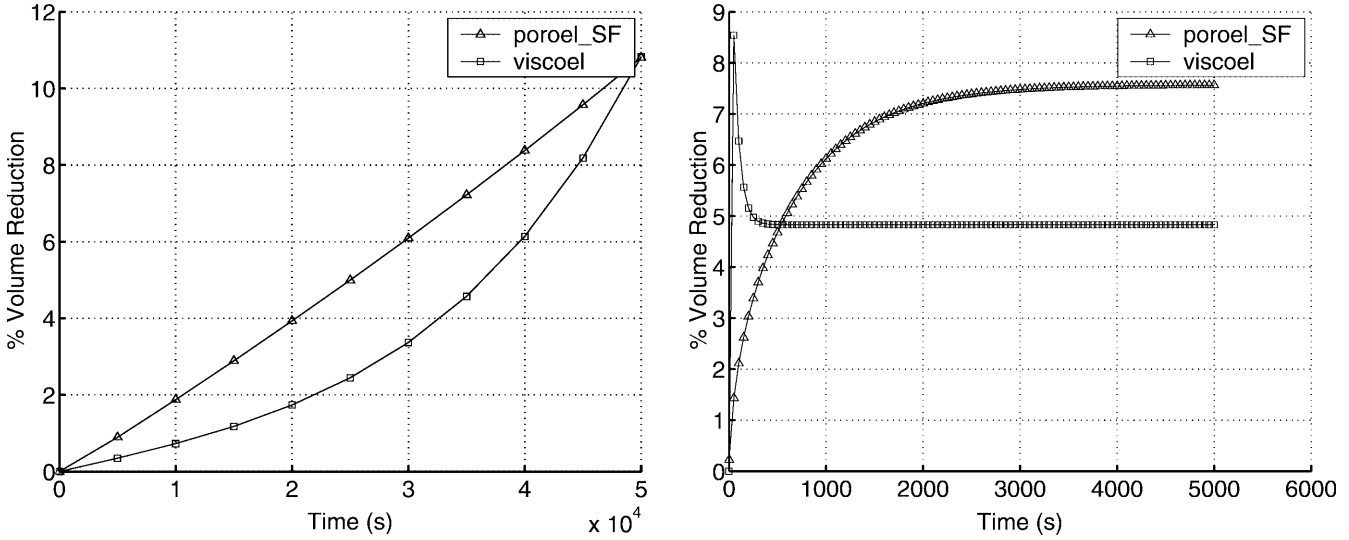

Fig. 5. The viscoelastic model behavior with the addition of a compressibility constant $D_{10} = 0.00110\ \text{Pa}^{-1}$. Left: Comparison of the poroelastic and viscoelastic compressibility under slow constant speed. Right: Similar to left, but for stress relaxation. Both plots show quite a different compressibility behavior: in particular, the relaxation behavior is totally different with the poroelastic model having a logarithmic-type compressibility while the viscoelastic model has more of a relaxation behavior, with a spike at the origin and then a smoothly converging reduction

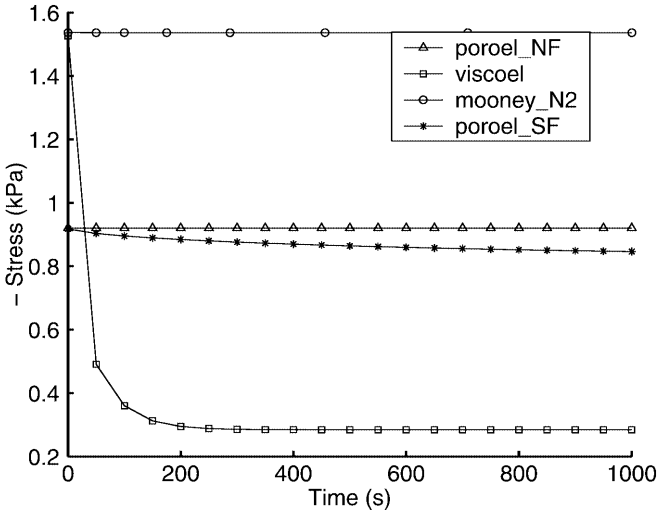

Fig. 6. Cauchy stress vs time in a stress relaxation simulation. The viscoelastic model has a far stronger relaxation behavior than the poroel_SF. This indicates that a poroelastic material may not be suitable to model the relaxation properties of brain tissue. A more advanced poro-viscoelastic model may be required. As expected, both the poroel_NF and the mooney_N2 do not change with time after the initial peak and are included only for comparison

relaxation can be reproduced using a poroelastic theory (Barry and Aldis 1992). Yang and Taber (1991) advocate the use of poroelasticity (together with some viscoelastic elements) in modeling the passive cardiac muscle. However, one of their conclusions is that the hysteresis produced by the poroelastic model (with no viscous elements) was much smaller than the experimental one. The need for a viscoelastic solid within a poroelastic formulation has also been reported within the articular cartilage research community (see for example (DiSilvestro et al. 2001) and references therein). It thus seems that poroelastic models may not be appropriate for modeling some moderate-strain-rate surgical manipulations. Nevertheless, they may be more appropriate for low-strain-rate situations, e.g. structural diseases like hydrocephalus or for brain hemorrhage modeling. In conclusion, a poro-viscoelastic model which would combine the advantages of both poroelastic and viscoelastic models may ultimately be needed.

We have found that a compressible viscoelastic model has a different mode of volume reduction compared to the poroelastic one with the volume reduction being highest at time zero and decreasing fast to an equilibrium state. On the other hand, the poroelastic model has zero volume reduction early on and increases fast to the equilibrium state. We also note that the compressibility of the poroelastic material, when no fluid is allowed to leave the specimen, is practically zero even though it has a Poisson's ratio $\nu = 0.35$. This should be a clarification of the fact that the ν is based on the **dry** material and that both the solid and fluid parts of the poroelastic mixture are incompressible.

We have used a constant permeability and have not allowed changes in its value due to compression of the voids. As an example, the permeability should intuitively be significantly reduced when the material is under large compressive strains. The use of constant permeability may thus be an important source of error and indicates that further evaluation would be of value. The need for a variable permeability in the poroelastic formulation has also been discussed extensively before (Kaczmarek et al. 1997; Barry and Aldis 1992).

We have performed some preliminary calculations on the effect of gravity using the instantaneous and long-term elastic moduli of the viscoelastic model; these show a strain of approximately 0.05–0.10 which indicates that it should not be neglected. Thus, we suggest that since brain tissue is in a physiological no-gravity environment, experiments on quasi-static brain tissue should be performed with the tissue immersed in saline or artificial CSF solution. By performing such experiments in air, we may obtain misleading results for the various elastic moduli.

References

ABAQUS (2001). Version 6.2. Hibbit, Karlsson, and Sorensen, Inc., USA.

Akkas, N.: Continuum modeling of head injury. Progress in Biomechanics, Ed. N. Akkas, (1979) 297–331

Bandak, F.A.; Vander Vorst, M.J.; Stuhmiller, L.M.; Mlakar, P.F.; Chilton, W.E.; Stuhmiller, J.H.: An imaging-based computational and experimental study of skull fracture: finite element model development. [Review]. J Neurotrauma 12(4) (1995) 679–88

Barry, S.I.; Aldis, G.K.: Flow-induced deformation from pressurized cavities in absorbing porous tissues. Bulletin of Mathematical Biology 54 (1992) 977–97

Basser, P.J.: Interstitial pressure, volume, and flow during infusion into brain tissue. Microvascular Research 44 (1992) 143–65

Bilston, L.E.; Liu, Z.; Phan-Thien, N.: Linear viscoelastic properties of bovine brain tissue in shear. Biorheology 34 (1997) 377–85
Chinzei, K.; Miller, K.: Compression of swine brain tissue; experiments in vitro. J Mech Eng Laboratory 50(4) (1996) 106–115
DiSilvestro, M.R.; Zhu, Q.; Wong, M.; Jurvelin, J.S.; Suh, J.K.: Biphasic poroviscoelastic simulation of the unconfined compression of articular cartilage: I–Simultaneous prediction of reaction force and lateral displacement. J Biomech Eng 123(2) (2001) 191–7
Donnelly, B.R.; Medige, J.: Shear properties of human brain tissue. J Biomech Eng 119(4) (1997) 423–32
Ferrant, M.; Warfield, S.K.; Nabavi, A.; Jolesz, F.A.; Kikinis, R.: Registration of 3D intraoperative MR images of the brain using a finite element biomechanical model. MICCAI 2000 Proceedings, Pittsburg, (2000) 19–28
Goldsmith, W.: Biomechanics of head injury. In Y. Fung, N. Perrone, and M. Anliker (Eds.), Symposium on Biomechanics, its Foundations and Objectives (1970 : University of California, San Diego), (1972) pp. 585–635. Prentice-Hall, Englewood Cliffs, N.J.
Guillaume, A.; Osmont, D.; Gaffie, D.; Sarron, J.C.; Quandieu, P.: Effects of perfusion on the mechanical behavior of the brain-exposed to hypergravity. J Biomech 30(4) (1997) 383–9
Hartmann, U.; Kruggel, F.: Transient analysis of the biomechanics of the human head with a high-resolution 3D finite element model. Comput Methods Biomech Biomed Eng 2(1) (1999) 49–64
Kaczmarek, M.; Subramaniam, R.P.; Neff, S.R.: The hydromechanics of hydrocephalus: Steady-state solutions for cylindrical geometry. Bulletin of Mathematical Biology 59 (1997) 295–323
King, A.I.; Ruan, J.S.; Zhou, C.; Hardy, W.N.; Khalil, T.B.: Recent advances in biomechanics of brain injury research: a review. J Neurotrauma 12(4) (1995) 651–8
Kyriacou, S.K.; Davatzikos, C.A.: A biomechanical model of soft tissue deformation, with applications to non-rigid registration of brain images with tumor pathology. Medical Image Computing and Computer-Assisted Intervention – MICCAI'98, Lecture Notes in Computer Science, Vol. 1496, (1998) 531–538
Kyriacou, S.K.; Davatzikos, C.; Zinreich, S.J.; Bryan, R.N.: Nonlinear elastic registration of brain images with tumor pathology using a biomechanical model. IEEE Trans on Med Imag 18 (1999) 580–592
Manduca, A.; Oliphant, T.E.; Dresner, M.A.; Mahowald, J.L.; Kruse, S.A.; Amromin, E.; Felmlee, J.P.; Greenleaf, J.F.; Ehman, R.L.: Magnetic resonance elastography: non-invasive mapping of tissue elasticity. Med Image Anal 5(4) (2001) 237–54
Mendis, K.K.; Stalnaker, R.; Advani, S.H.: A constitutive relationship for large-deformation finite-element modeling of brain-tissue. J Biomech Eng Trans ASME 117 (1995) 279–285
Metz, H.; McElhaney, J.; Ommaya, A.K.: A comparison of the elasticity of live, dead, and fixed brain tissue. J Biomech 3 (1970) 453–458
Miga, M.I.; Paulsen, K.D.; Hoopes, P.J.; Jr. Kennedy, F.E.; Hartov, A.; Roberts, D.W.: In vivo quantification of a homogeneous brain deformation model for updating preoperative images during surgery. IEEE Trans Biomed Eng 47(2) (2000) 266–73
Miga, M.; Paulsen, K.; Kennedy, F.; Hoopes, J.; Hartov, A.; Roberts, D.: Initial in-vivo analysis of 3D heterogeneous brain computations for model-updated image-guided neurosurgery. Lec Notes in Comp Sci: Proc of MICCAI'98 1496 (1998a) 742–752
Miga, M.I.; Paulsen, K.D.; Kennedy, F.E.; Hoopes, P.J.; Hartov, A.; Roberts, D.W.: Modeling surgical loads to account for subsurface tissue deformation during stereotactic neurosurgery. IEEE SPIE Proceedings of laser-tissue interaction IX, Part B: Soft tissue modeling 3254, (1998b) 501–11
Miller, K.: (1998). Modelling soft tissue using biphasic theory – a word of caution. Comput Meth Biomech Biomed Eng 1, 261–3
Miller, K.: Constitutive model of brain tissue suitable for finite element analysis of surgical procedures. J Biomech 32 (1999) 531–37
Miller, K.; Chinzei, K.: Constitutive modelling of brain tissue – experiment and theory. J Biomech 30, (1997) 1115–1121
Miller, K.; Chinzei, K.; Orssengo, G.; Bednarz, P.: Mechanical properties of brain tissue in-vivo: experiment and computer simulation. J Biomech 33 (2000) 1369–76
Nagashima, T.; Shirakuni, T.; Rapoport, S.I.: A two-dimensional, finite element analysis of vasogenic brain edema Neurol Med Chir 30(1) (1990) 1–9
Nagashima, T.; Tada, Y.; Hamano, S.; Skakakura, M.; Masaoka, K.; Tamaki, N.; Matsumoto, S.: The finite element analysis of brain oedema associated with intracranial meningiomas. Acta Neurochir Suppl (Wien) 51 (1990) 155–7
Nagashima, T.; Tamaki, N.; Matsumoto, S.; Horwitz, B.; Seguchi,Y.: Biomechanics of hydrocephalus: A new theoretical model. Neurosur 21(6) (1987) 898–904
Nagashima, T.; Tamaki, N.; Takada, M.; Tada, Y.: Formation and resolution of brain edema associated with brain tumors. A comprehensive theoretical model and clinical analysis. Acta Neurochir Suppl (Wien) 60 (1994) 165–7
Ommaya, A.K.: Mechanical properties of tissues of the nervous system. J Biomech 1 (1968) 127–38
Ozawa, H.; Matsumoto, T.; Ohashi, T.; Sato, M.; Kokubun, S.: Comparison of spinal cord gray matter and white matter softness: measurement by pipette aspiration method. J Neurosurg 95(2 Suppl), (2001) 221–4
Paulsen, K.D.; Miga, M.I.; Kennedy, F.E.; Hoopes, P.J.; Hartov, A.; Roberts, D.W.: A computational model for tracking subsurface tissue deformation during stereotactic neurosurgery. IEEE Trans Biomed Eng 46(2) (1999) 213–25
Pena, A.; Bolton, M.D.; Whitehouse, H.; Pickard, L.D.: Effects of brain ventricular shape on periventricular biomechanics: A finite-element analysis. Neurosur 45(1) (1999) 107–116

Prange, M.T.; Meaney, D.F.; Margulies, S.S.: Defining brain mechanical properties: effects of region, direction, and species. Stapp Car Crash J 44(Nov.) (2000) 205–13
Roberts, D.W.; Hartov, A.; Kennedy, F.E.; Miga, M.I.; Paulsen, K.D.: Intraoperative brain shift and deformation: A quantitative analysis of cortical displacement in 28 cases. Neurosur 43 (1998) 749–758
Sahay, K.B.; Mehrotra, R.; Sachdeva, U.; Banerji, A.K.: Elastomechanical characterization of brain tissues. J Biomech 25 (1992) 319–326
Sarron, J.C.; Blondeau, C.; Guillaume, A.; Osmont, D.: Identifcation of linear viscoelastic constitutive models. J Biomech (2000)
Shuck, L.Z.; Advani, S.H.: Rheological response of human brain tissue in shear. J Basic Eng 12 (1972) 905–11
Skrinjar, O.M.; Duncan, J.S.: Real time 3D brain shift compensation. Lect. Notes in Comp. Sci.: IPMI 99 1613 (1999) 42–55
Skrinjar, O.M.; Studholme, C.; Nabavi, A.; Duncan, J.S.: Steps toward a stereo-camera-guided biomechanical model for brain shift compensation. Lect. Notes in Comp. Sci.:IPMI 2001 (2001) 183–189

Subramaniam, R.P.; Neff, S.R.; Rahulkumar, P.: A numerical study of the biomechanics of structural neurologic diseases. In A. Tentner (Ed.), High Performance Computing-Grand Challenges in Computer Simulation Society for Computer Simulations, San Diego, (1995) pp. 552–60
Takizawa, H.; Sugiura, K.; Baba, M.; Miller, J.D.: Analysis of intracerebral hematoma shapes by numerical computer simulation using the finite element method. Neurologia Medico-Chirurgica 34 (1994) 65–9
Tenti, G.; Sivaloganathan, S.; Drake, J.M.: Brain biomechanics: Steady state consolidation of hydrocephalus. Canadian Applied Mathematics Quarterly 7(1) (1999) 111–124
Wang, H.C.; Wineman, A.S.: A mathematical model for the determination of viscoelastic behavior of brain in vivo. I. Oscillatory response. J Biomech 5(5) (1972) 431–46
Wasserman, R.; Acharya, R.: A patient-specific in vivo tumor model. [Review]. Mathematical Biosci 136(2) (1996) 111–40
Yang, M.; Taber, L.A.: The possible role of poroelasticity in the apparent viscoelastic behavior of passive cardiac muscle. J Biomech 24 (1991) 587–97
Yundt, K.D.; Grubb, R.L.; Diringer, Jr. M.N.; Powers, W.J.: Cerebral hemodynamic and metabolic changes caused by brain retraction after aneurysmal subarachnoid hemorrhage. Neurosurgery 40 (1997) 442–50
Zhou, C.; Khalil, T.B.; King, A.I.: Shear stress distribution in the porcine brain due to rotational impact. Proc. 38th Stapp Car Crash Conference, SAE, Ft. Lauderdale, FL. SAE Paper No. 942214, 133 (1994)